Polyketides from Marine Dinoflagellates of the Genus *Prorocentrum*, Biosynthetic Origin and Bioactivity of Their Okadaic Acid Analogues

Weimin Hu[1], Jing Xu[2], Jari Sinkkonen[3] and Jun Wu*[,1]

[1]*Key Laboratory of Marine Bio-resources Sustainable Utilization, South China Sea Institute of Oceanology, Chinese Academy of Sciences, 164 West Xingang Road, Guangzhou 510301, China*

[2]*School of Medicine and Pharmacy, Ocean University of China, Qingdao 266003, China*

[3]*Laboratory of Organic Chemistry and Chemical Biology, Department of Chemistry, University of Turku, Turku 20014, Finland*

Abstract: Marine dinoflagellates of the genus *Prorocentrum* are famous for the production of okadaic acid (OA) and its analogues. This review covers first the source, chemistry and bioactivity of polyketides from *Prorocentrum* species. Then recent advances in the studies of biosynthetic origin of OA and its analogues are included. Moreover, the pharmacophore for the selective inhibition of OA to protein phosphatases types 1 (PP1) and 2A (PP2A) is highlighted.

Keywords: Dinoflagellate, *Prorocentrum*, polyketide, okadaic acid, biosynthetic origin, inhibition to PP1 and PP2A, pharmacophore.

1. INTRODUCTION

Marine dinoflagellates of the genus *Prorocentrum* are famous for the production of okadaic acid (OA) and its analogues, which are inhibitors of protein phosphatases type 1 (PP1) and 2A (PP2A), and causative toxins of diarrhetic shellfish poisoning (DSP). The wide geographic occurrence of this poisoning poses serious threats to both human health and shellfish industries. The toxins responsible for DSP are mainly OA and its analogues, such as dinophysistoxins (DTXs, i.e. DTX-1, -2) and OA esters. OA, characterized as the main secondary metabolite of *Prorocentrum* species, is the first example of polyether toxins known as a highly selective inhibitor of PP1 and PP2A, and a potent tumor promoter. To date, twenty-six OA analogues and ten other polyketides have been identified from the dinoflagellates of the genus *Prorocentrum*, including *P. arenarium*, *P. belizeanum*, *P. concavum*, *P. faustiae*, *P. hoffmannianum*, *P. lima*, and *P. maculosum*. This review covers first the source, chemistry and bioactivity of polyketides from *Prorocentrum* species. After that the recent advances in the biosynthetic origin studies of OA and its analogues are included. In addition, the pharmacophore for the selective inhibition of OA to PP1 and PP2A is highlighted.

2. POLYKETIDES

2.1. OA and its Analogues

OA, a cytotoxic polyether derivative of a C_{38} fatty acid, was first isolated independently in 1981 from two sponges, *Halichondria okadai* Kadota, a black sponge commonly found along the Pacific coast of Japan, and *H. melanodocia*, a Caribbean sponge collected in the Florida Keys [1]. It was found to be toxic for mammal (LD_{50} = 192 μg/kg, i.p. mice) and able to inhibit the growth of a human nasopharyngeal carcinoma cell line KB by more than 80% at 5 ng/mL. Its structure and the absolute configuration were unambiguously established by X-ray crystallography of its *o*-bromobenzyl ester [1]. During the same year, also its 9, 10-α-episulfide derivative, named acanthifolicin, identified from the marine sponge *Pandaros acanthifolium* by X-ray crystallography [2]. One year later, OA was characterized as a toxic component from the marine dinoflagellate *P. lima*, isolated at Tahiti Island [3]. It was the first time when the origin of OA was disclosed from marine dinoflagellate. Dinophysistoxin-1 (DTX-1), previously characterized from the dinoflagellate *Dinophysis fortii*, was later also found in *P. lima* and *P. faustiae* [4-6]. To date, altogether twenty-six OA analogues have been identified from the dinoflagellates of the genus *Prorocentrum* [3-24]. They can be classified into two groups, one comprising compounds with different substituents or conformational change on the skeleton of OA (**1-4**, **23-26**, see Tables **1-3**) and another including the different long chain esters at the carboxyl group of OA (**5-22**). Among the above OA analogues, DTX-1 (LD_{50} = 160 μg/kg, i.p. mice) [25-26] and DTX-2 (LD_{50} = 338 μg/kg, i.p. mice) [27] have been found to be the most toxic.

2.2. Other Polyketides

To date, ten other polyketides without OA carbon framework have been identified from dinoflagellates of the genus *Prorocentrum* (**27-36**, see Table **4**). Prorocentrolide (**27**), a toxic macrocycle with a C_{27} macrolide and a hexahydroisoquinoline group moiety as a part of the molecule, was the first one characterized from *P. lima*. It had a mouse

*Address correspondence to these authors at the Key Laboratory of Marine Bio-resources Sustainable Utilization, South China Sea Institute of Oceanology, Chinese Academy of Sciences, 164 West Xingang Road, Guangzhou 510301, China; Tel: +86-20-84458442; Fax: +86-20-84451672; E-mail: wwujun2003@yahoo.com

1389-5575/10 $55.00+.00

Table 1. Structures of 1-23

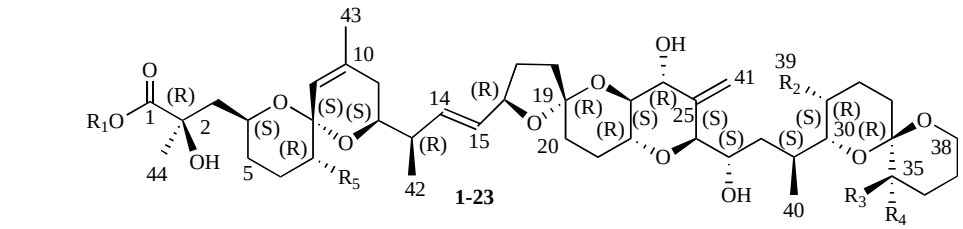

1-23

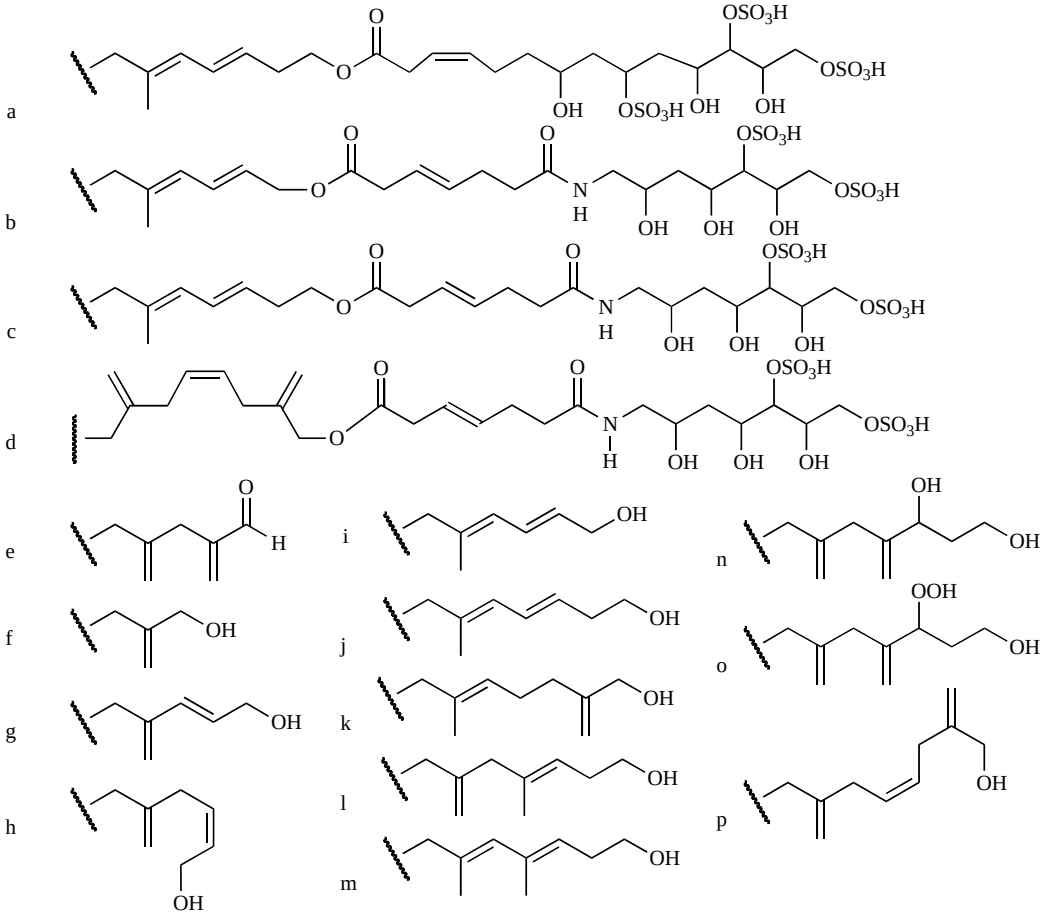

No.	Name	R_1	R_2	R_3	R_4	R_5	Species	Refs.
1	OA	H	CH_3	H	H	OH	*P.lima, P.arenarium, P.belizeanum, P.concavum, P.faustiae, P.maculosum*	[3-8]
2	19-epi OA (19-*R*)	H	CH_3	H	H	OH	*P.belizeanum*	[9]
3	DTX-1	H	CH_3	CH_3	H	OH	*P.lima, P.faustiae*	[4-5, 10]
4	DTX-2	H	H	H	CH_3	OH	*P.lima*	[4, 11]
5	DTX-4	**a**	CH_3	H	H	OH	*P.lima, P.muculosum*	[12, 13]
6	DTX-5a	**b**	CH_3	H	H	OH	*P.muculosum*	[14]
7	DTX-5b	**c**	CH_3	H	H	OH	*P.maculosum*	[14]
8	DTX-5c	**d**	CH_3	H	H	OH	*P.belizeanum*	[7]
9	DTX-6	**e**	CH_3	H	H	OH	*P.lima*	[15]
10	C_4-diol OA	**f**	CH_3	H	H	OH	*P.lima*	[16]

(Table 1). Contd…..

No.	Name	R_1	R_2	R_3	R_4	R_5	Species	Refs.
11	C_6-diol OA	**g**	CH_3	H	H	OH	*P.lima*	[17]
12	C_7-diol OA	**h**	CH_3	H	H	OH	*P.lima*	[18]
13	C_7-diol OA	**i**	CH_3	H	H	OH	*P.maculosum*	[4]
14	C_8-diol OA	**j**	CH_3	H	H	OH	*P.lima, P.maculosum*	[4]
15	C_9-diol OA	**k**	CH_3	H	H	OH	*P.lima*	[19]
16	C_9-diol OA	**l**	CH_3	H	H	OH	*P.lima*	[4, 20]
17	C_9-diol OA	**m**	CH_3	H	H	OH	*P.lima*	[21]
18	C_9-diol OA	**n**	CH_3	H	H	OH	*P.lima*	[17]
19	C_9-diol OA	**o**	CH_3	H	H	OH	*P.lima*	[17]
20	C_{10}-diol OA	**p**	CH_3	H	H	OH	*P.belizeanum*	[17]
21	Methyl OA	CH_3	CH_3	H	H	OH	*P.maculosum, P.lima*	[4]
22	Ethyl OA	Ethyl	CH_3	H	H	OH	*P.lima*	[4]
23	7-deoxy OA	H	CH_3	H	H	H	*P.lima*	[22, 23]

Abbreviations: Okadaic acid (OA); Dinophysistoxin (DTX).

Table 2. Structures of 24-25

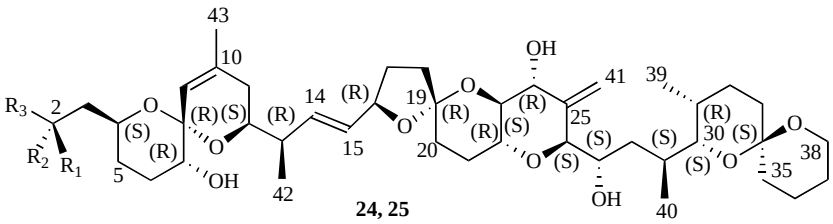

24, 25

No.	Name	R_1	R_2	R_3	Species	Refs.
24	2-deoxy OA	H	CH_3	COOH	*P.lima*	[22]
25	Norokadanone	=O		CH_3	*P.lima*	[16]

Table 3. Structures of 26

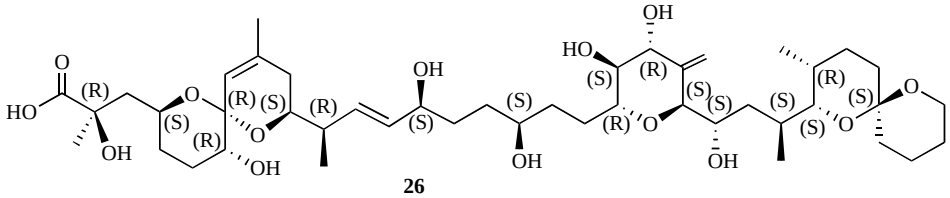

26

No.	Name	Species	Ref.
26	Belizeanic acid	*P.belizeanum*	[24]

lethality of 0.4 mg/kg (LD_{50} i.p.) and its biosynthetic precursor was proposed to be a C_{49} fatty acid [28]. Three prorocentrolide derivatives, 9,51-dihydroprorocentrolide (**28**), prorocentrolide 30-sulfate (**29**), and 4-hydroxyprorocentrolide (**30**), were identified later from *P. lima* [29]. A macrolide possessing a spiro-linked cyclic imine group with an *ortho*, *para*-disubstituted 3′-cyclohexene, named spiroprorocentrimine (**31**), was obtained as a polar lipid-soluble

Table 4. Structures of 27-36

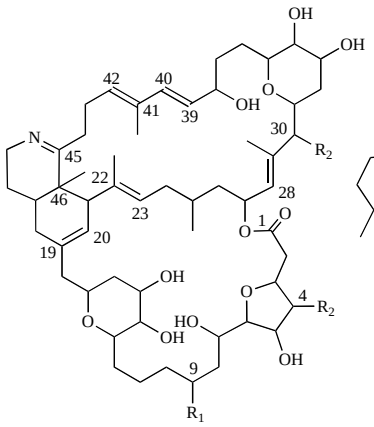

27-30

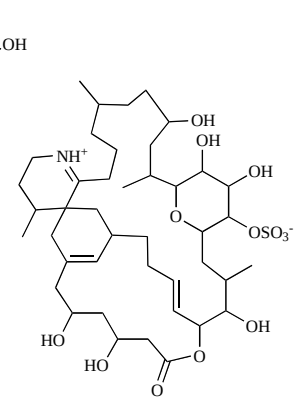

31

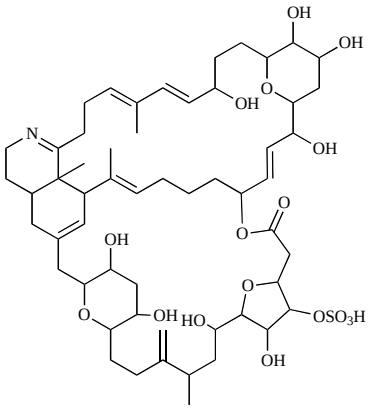

32

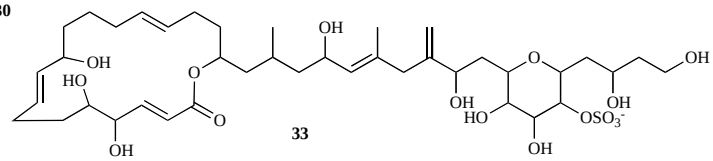

33

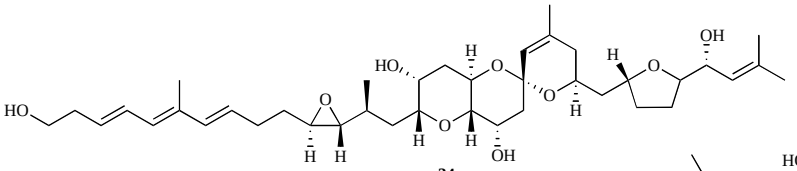

34

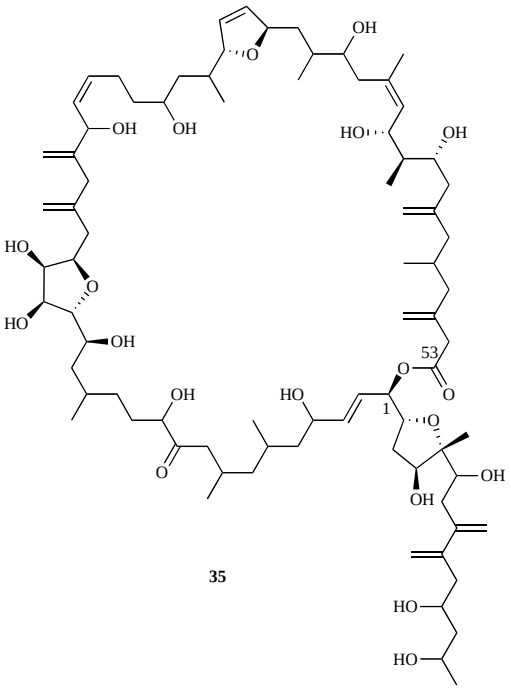

35

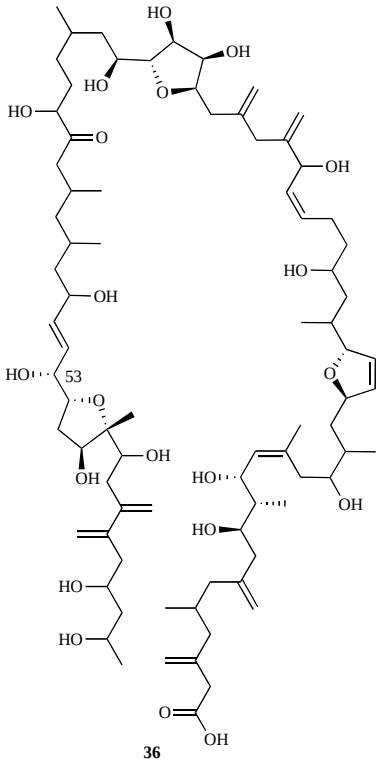

36

No.	Name	R_1	R_2	R_3	Species	Refs.
27	Prorocentrolide	$=CH_2$	H	H	*P.lima*	[28, 30]
28	9,51-dihydroprorocentrolide	CH_3	H	H	*P.lima*	[29]
29	Prorocentrolide 30-sulfate	$=CH_2$	H	OSO_3H	*P.lima*	[29]

(Table 4). Contd…..

No.	Name	R_1	R_2	R_3	Species	Refs.
30	4-hydroxyprorocentrolide	$=CH_2$	OH	H	*P.lima*	[30]
31	spiro-prorocentrimine	-	-	-	*P.sp.*	[30]
32	Prorocentrolide B	-	-	-	*P.maculosum*	[31]
33	Hoffmanniolide	-	-	-	*P.hoffmannianum*	[32]
34	Prorocentin	-	-	-	*P.lima*	[33]
35	Belizeanolide	-	-	-	*P.belizeanum*	[34]
36	Belizeanolic acid	-	-	-	*P.belizeanum*	[34]

toxin from the laboratory-cultured benthic *Prorocentrum* species collected at Taiwan. Its relative configuration was established by single-crystal X-ray diffraction analysis. The mouse toxicity assay (i.p.) of **31** exhibited an LD_{99} value of 2.5 mg/kg [30]. Prorocentrolide B (**32**), a fast-acting toxin, was isolated from the *n*-BuOH extract of the tropical dinoflagellate *P. maculosum.* The relative configurations of the five- and six-membered rings of the molecule were established by NMR and mass spectra [31]. A nineteen-membered macrocyclic polyether lactone, hoffmanniolide (**33**), was obtained from *P. hoffmannianum* and its planar structure was elucidated. However, it showed no evidence of cytotoxicity up to the concentration of 100 μg/ml [32]. Prorocentin (**34**) characterized from *P. lima*, was collected from the wash-off epiphytes of seaweeds growing in the coral reef of Taiwan [33]. Recently, belizeanolide (**35**), an unprecedented class of polyunsaturated and polyhydroxylated macrocycle possessing a backbone with sixty-six carbon atoms that includes a unique fiftyfour -membered lactone containing two furan-type rings, was identified from the marine dinoflagellate *P. belizeanum*, together with its open form, belizeanolic acid (**36**). Both compounds showed significant antiproliferative activities. The GI_{50} (μM) values for belizeanolide were 3.28 ± 0.45 (A2780), 3.23 ± 0.45 (SW1573), 3.23 ± 0.38 (HBL100), 3.16 ± 0.40 (T47D), and 4.58 ± 0.40 (WiDr). However, it is noteworthy that the open compound belizeanolic acid is ten times more potent than belizeanolide. Its GI_{50} (μM) values were 0.26 ± 0.09 (A2780), 0.31 ± 0.06 (SW1573), 0.32 ± 0.04 (HBL100), 0.40 ± 0.09 (T47D), and 0.41 ± 0.04 (WiDr) [34].

3. BIOSYNTHETIC ORIGIN OF OA AND ITS ANALOGUES

3.1. ^{13}C-Labeling Patterns of OA and DTX-1

The carbon origin of OA and DTX-1 was investigated by ^{13}C-labeled precursor incorporation experiments and their ^{13}C-incorporation patterns were analyzed by NMR spectroscopy. Initially, the carbon biosynthetic origin of OA and DTX-1 was evaluated by the incorporation of ^{13}C-labeled precursors, [1-^{13}C], [2-^{13}C], and [1, 2-^{13}C]acetate. The results showed that all the carbons except C-37 and C-38 originated from acetate and sixteen acetate units were observed to be incorporated into the structures of OA and DTX-1 (Fig. **1a**) [35]. However, the origin of C-37 and C-38 was proved to be from glycolate [36]. It should be noted that all the pendant methyl groups of OA and DTX-1 were derived from the methyl group of acetate. Fragments A (C-1 to C-7 and C-44), C (C-11 to C-22 and C-42), and E (C-27 to C-36 and C-39, C-40) were biosynthesized *via* a classical polyketide path-

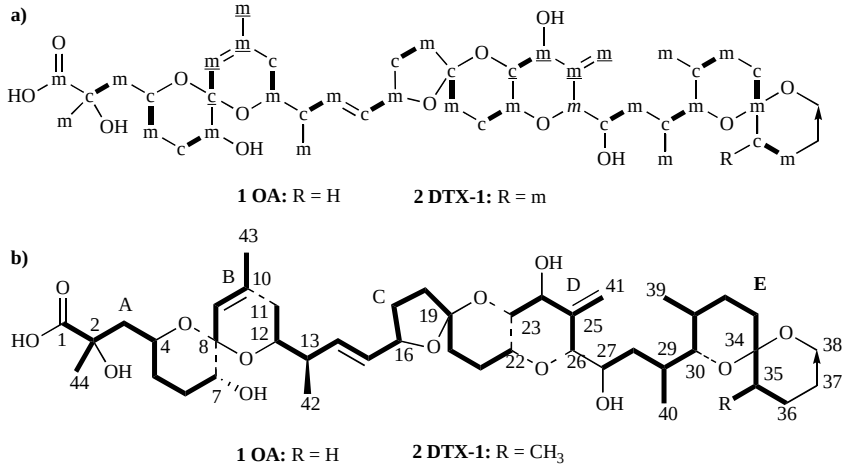

Fig. (1). ^{13}C-labeling patterns of OA and DTX-1. **a**) underlined fragments: nonclassical polyketide units, **m**: C-atom originates from an acetate methyl group, **c**: C-atom originates from an acetate carboxyl group, **c-m**: C-atoms originate from an acetate unit, ↑: glycolate; **b**) Bold lines show the different fragments proposed; A, C, and E: polyketide chain; B and D: unknown pathway; ↑: carbons from glycolate.

way. However, fragments B (C-8 to C-10 and C-43) and D (C-23 to C-26 and C-41) originated from an unknown biogenetic pathway (Fig. **1b**) [37], in which a series of Favorskii rearrangements were invoked to eject the carbonyl carbon of an intact polyketide acetate unit, resulting in a series of 'isolated' backbone carbons derived only from the methyl group of a cleaved acetate unit. Later, a quantitative comparison of peak intensities between the ^{13}C NMR spectra of OA labeled with [2-$^{13}C_1$] sodium butyrate and [2-$^{13}C_1$] sodium acetate showed a clear difference of the signal intensities corresponding to C-3, C-14, C-18, C-22, C-30, and C-34. The extra enriched intensity of these carbons was observed upon labeling with [2-$^{13}C_1$] sodium butyrate. It was suggested that the biogenetic origin of OA and its analogues could be rationalized considering the use of more evolved fragments with four or more carbons as intermediates, such as acetoacetyl or glutaconyl-CoA [37].

3.2. ^{18}O-Labeling Pattern of OA

The oxygen origin of OA was investigated by ^{18}O-labeled precursor incorporation experiments and the ^{18}O-incorporation patterns of OA were analyzed by collision-induced dissociation tandem mass spectrometry (CID MS/MS). The extensive determination of $^{18}O/^{16}O$ ratios for each product ion bearing different numbers of incorporated ^{18}O atoms resulted in the complete assignment of the labeled positions with accurate isotope ratios. The oxygen atoms labeled from molecular oxygen ($^{18}O_2$) were O(1)/O(2), O(3), O(5), O(6), O(8), O(9), O(10), and O(12) (Fig. **2**). However, those labeled from [$^{18}O_2$]acetate were O(4), O(6), O(7), and O(11) (Fig. **2**). These incorporation patterns suggested that the cyclization of ether rings C, D, and E occurred *via* a β-epoxide intermediate at C22-C23, and the carboxylic acid was formed by the Baeyer-Villiger oxidation [38]. The oxygen positions labeled from $H_2{}^{18}O$ were O(1), O(2), O(5), O(6), O(7), O(10), O(12), and O(13), and their incorporating ratios were more than 7% (Fig. **2**). Oxygen atoms O (4) and O (11), derived from acetate, were not labeled from $H_2{}^{18}O$. This could not be explained by the usual metabolic route where acetyl-CoA was biosynthesized *via* pyruvate. The above results implied that an oxidation mechanism other than those in actinomycetes polyethers might be involved in the biosynthesis of okadaic acid [39].

3.3. ^{13}C, ^{18}O and ^{2}H-Labeling Patterns of DTX-4, DTX-5a and DTX-5b

The structural difference between DTX-4 and the pair DTX-5a/5b resides in their sulfated side chains (Fig. **3**). The ^{13}C and ^{18}O-labeling patterns of the OA nucleus of DTX-4, DTX-5a and DTX-5b were the same as those of OA, whereas the ^{13}C, ^{18}O and ^{2}H-labeling patterns of DTX-4 confirmed a polyketide pathway, a Baeyer-Villiger oxidation step, and an unusual carbon deletion process derived from Favorski rearrangement in the biosynthesis of the sulfated side chain of DTX-4. The labeling work with DTX-4 clearly established that the side chain portion of the molecule is a polyketide chain incorporating a glycolate starting unit into which an oxygen atom is inserted to create an ester link (Fig. **3**) [40]. Similarly, this ester link was also present in the side chain of DTX-5a and DTX-5b. The length of the so-called diol ester moiety in DTX-4 and DTX-5b was the same. However, it was one carbon shorter in DTX-5a. The labeling data revealed that this was accounted for by the deletion of an acetate carboxyl carbon, presumably by a Favorski or Tiffeneau-Demyanov mechanism to yield a shorter chain by one carbon in DTX-5a (Fig. **3**). The amino acid residue in the sulfated side chain was found to originate from glycine, and oxygen insertion in the chain was shown to occur after the polyketide formation [41].

4. BIOACTIVITY

4.1. Inhibition to the Serine/Threonine Phosphatases PP1 and PP2A

In 1988, OA was reported to be the first highly selective inhibitor of the serine/threonine phosphatases PP1 and PP2A [42]. This discovery immediately revolutionized the ability to study of the role of protein phosphatases in cellular process. OA is 100-fold selective for PP2A over PP1 with IC_{50} = 0.2 nM and IC_{50} = 20 nM, respectively [43]. However, it inhibits the activity of PP2B, which is 40% identical to PP1 and PP2A with much lower potency (IC_{50} > 10 mM). It has no effect on unrelated phosphatases, such as PP2C and protein tyrosine phosphatases [44, 45].

4.1.1. PP1·OA Complex

The crystal structure of a PP1·OA complex to a resolution of 1.9Å was determined in 2001 [46]. Three grooves (hydrophobic, C-terminal and acidic) are on the surface of PP1. The structure reveals that OA binds in a hydrophobic groove adjacent to the active site of the protein of PP1 and interacts with basic residues within the active site. OA exhibits a cyclic structure, which is maintained *via* an intramolecular hydrogen bond between the C-24 hydroxy group and the C-1 acid. The double ring spiroketal moiety of OA is hydrophobic and binds into the hydrophobic groove

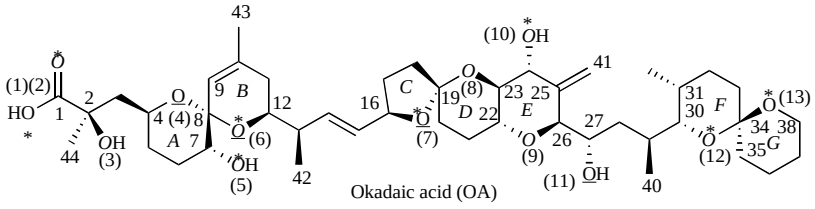

Fig. (2). ^{18}O-labeling pattern of okadaic acid. The italic oxygen atoms (*O*) are labeled from $^{18}O_2$ and underlined ones (O) from [$^{18}O_2$] acetate. ^{18}O-incorporation ratios: From $^{18}O_2$, one of O(1)/O(2) 11%, O(3) 7%, O(5) 15%, O(6) 14%, O(8) 15%, O(9) 19%, O(10) 8%, and O(12) 9%; from [$^{18}O_2$]acetate, O(4) 32%, O(6) 13%, O(7) 5%, and O(11) 31%(oxygen atoms are numbered beginning with those of carboxylic acid as O(1)/O(2) to O(13) in ring G). The asterisk ones (O*) are labeled from $H_2{}^{18}O$ and their incorporating ratios are more than 7%.

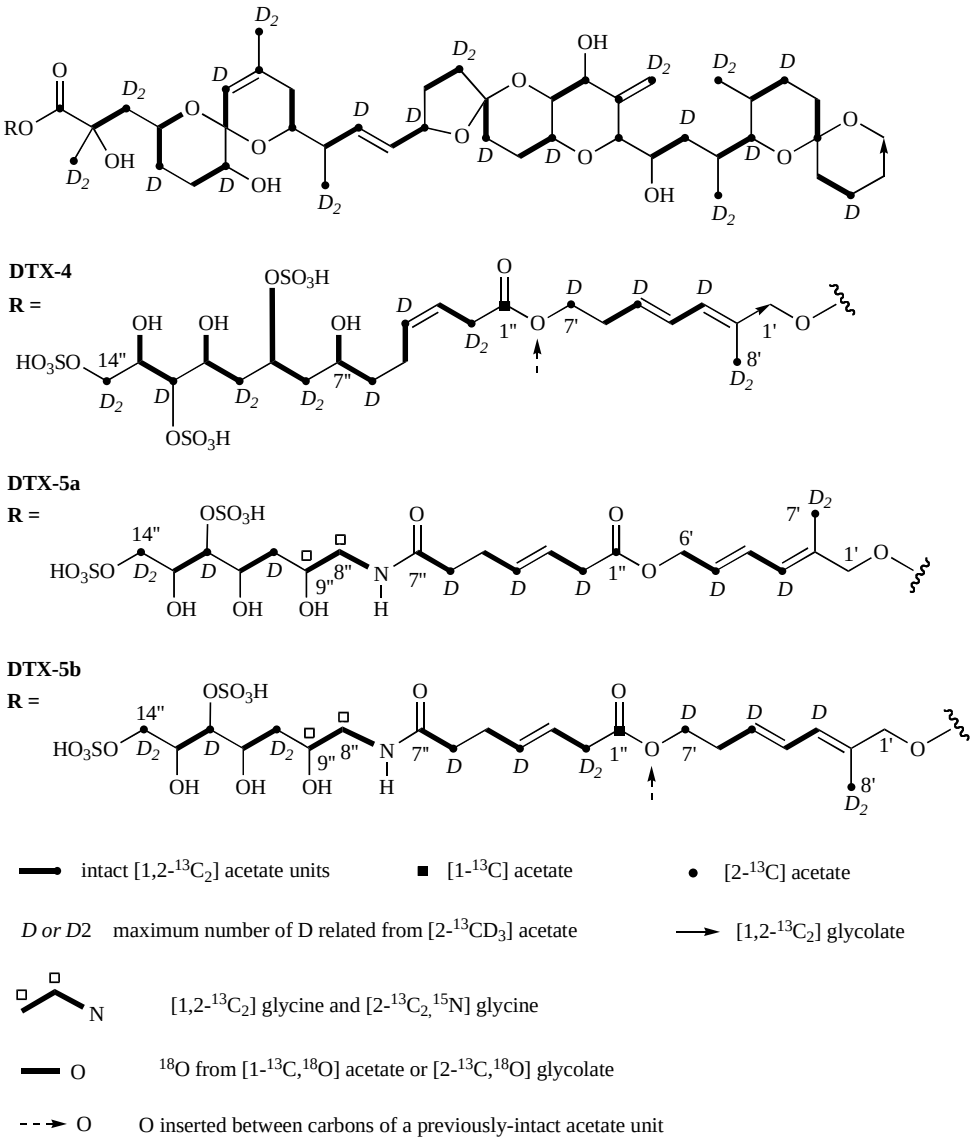

Fig. (3). ^{13}C, ^{18}O and D-labeling patterns of DTX-4, DTX-5a and DTX-5b.

on the surface of the PP1 protein. In the PP1·OA complex, Trp-206 and Ile-130 in the hydrophobic groove appear to be the two most important residues in this interaction due to their proximity to the hydrophobic segment of OA. Other hydrophobic interactions occur between the C-4 to C-16 region of OA and the PP1 residues Phe-276 and Val-250 (Fig. **4**). The remaining sites of interaction between PP1 and OA involve hydrogen bonding. The acid motif in OA accepts a hydrogen bond from the hydroxyl group of Tyr-272. Other hydrogen bonding interactions occur between Arg-96 and the C-2 hydroxy group of OA, and between Arg-221 and the C-24 hydroxy group of OA [46].

4.1.2. PP2A·OA Complex

The core enzyme of PP2A comprises a 36 kDa catalytic subunit and a 65 kDa scaffolding subunit. The crystal structure of a PP2A core enzyme bound to OA at 2.6 Å was determined in 2006 [47]. OA exhibits a cyclic structure derived from an intramolecular hydrogen bond between the C-24 hydroxy group and the C-1 acid as that in the PP1·OA complex. It binds to the active-site pocket of the catalytic subunit of PP2A. The double ring spiroketal moiety of OA binds into the hydrophobic cage in the catalytic subunit of PP2A. His-191 and Val-189 appear to be the two most important residues in this interaction (Fig. **5**). Hydrophobic interactions observed between the C9-C10 vinyl methyl group and the β12–β13 loop of PP2A residues are Cys266, Arg268, and Cys269. The residue Ile-123 interacts with the 44-methyl group. Other hydrophobic interactions occur between the C-12 to C-29 region of OA and the catalytic subunit residues Leu-243, Ile-123, Tyr-127, and Trp-200. The remaining sites of interaction between the catalytic subunit of PP2A and OA involve hydrogen bonding. The acid motif in OA accepts a hydrogen bond from the hydroxy group of Tyr-265. The residue Arg-89 exhibits two hydrogen bonding interactions with the C-2 hydroxy group and C-4 linked oxygen atom of OA, respectively. The other hydrogen bonding interaction

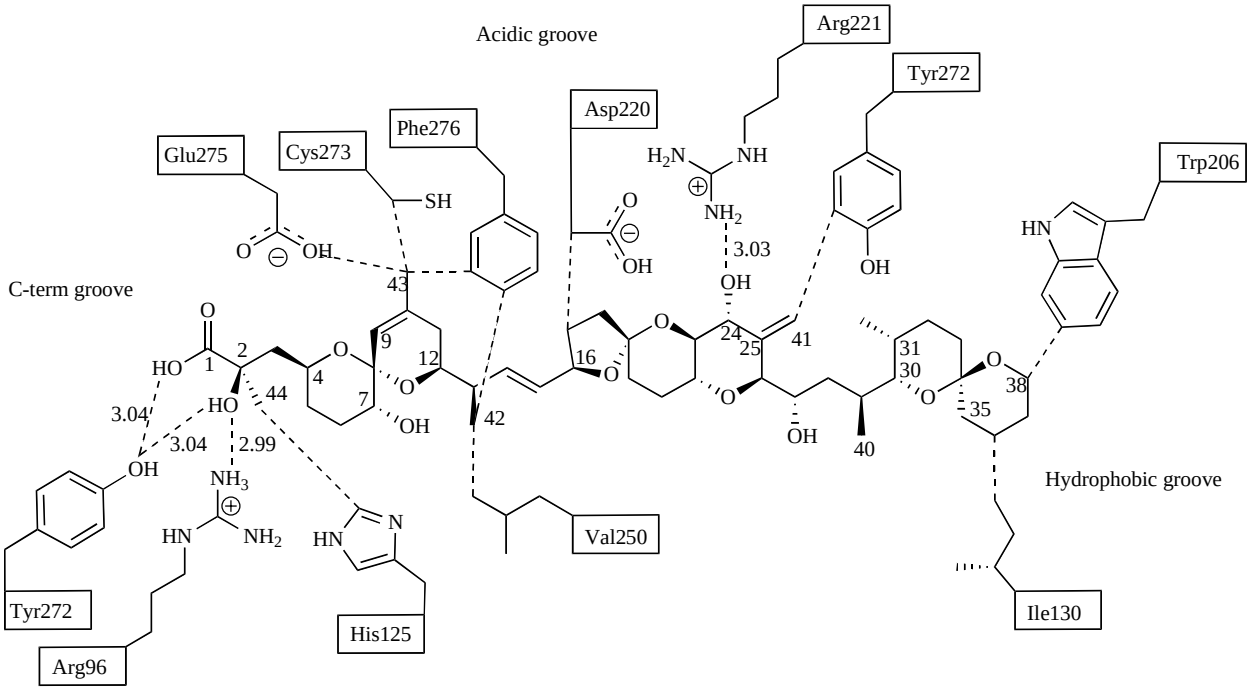

Fig. (4). Active sites of the PP1·OA complex. All residues of PP1 within 4Å of OA are shown (The closest residue-OA interactions are shown by dashed lines, and distances of all possible hydrogen bonding interactions are labeled).

occurs between Arg-214 and the C-24 hydroxy group of OA (Fig. **5**) [47].

Comparison of the structure of the PP2A·OA complex with that of PP1 bound to OA allowed rationalization of the strong preference of OA for PP2A. Although many residues of PP2A that specifically recognize OA are conserved in PP1, the hydrophobic cage in the catalytic subunit of PP2A that accommodates the hydrophobic end of OA is absent in PP1. His191, which resides on the intervening loop between helices α7 and α8 of PP2A, contributes to one side of the cage. Compared with His191, the corresponding residue Asp197 of the corresponding loop in PP1 is located 4–5 Å further away from OA. In addition, Gln122 of PP2A, whose aliphatic side chain contributes to another side of the hydro-

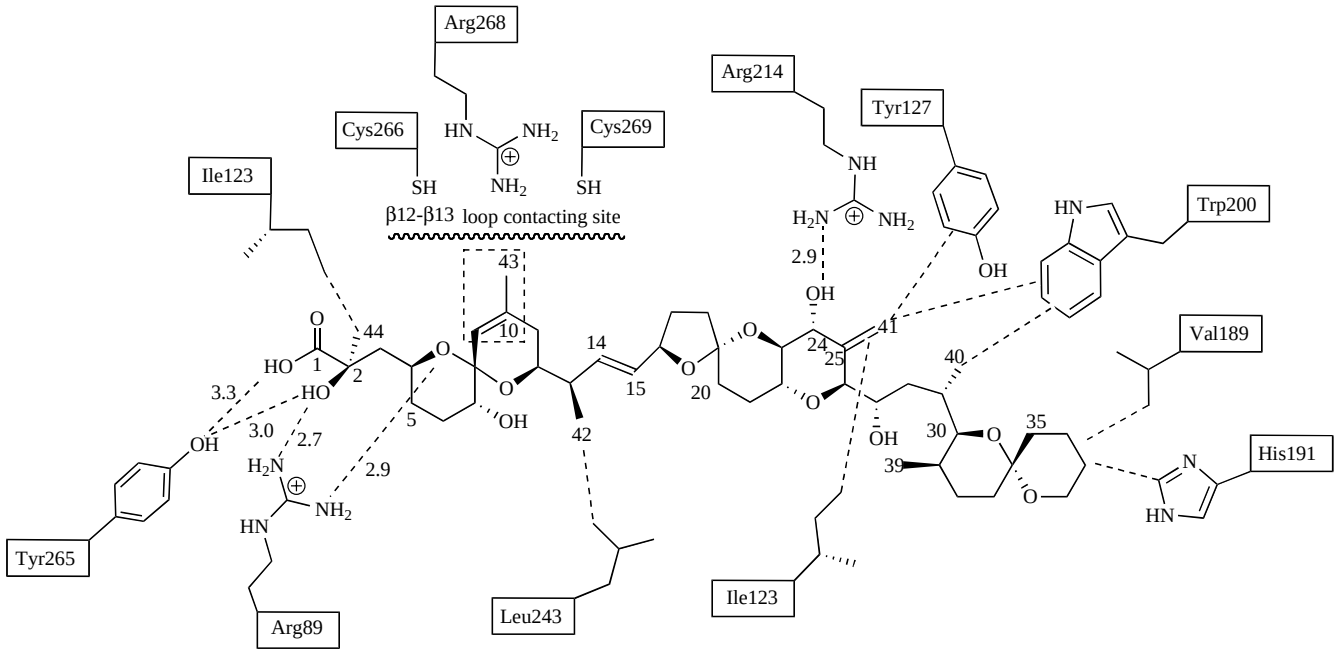

Fig. (5). Active sites of the PP2A·OA complex. All residues of PP2A within 4Å of OA are shown (The closest residue-OA interactions are shown by dashed lines, and distances of all possible hydrogen bonding interactions are labeled).

phobic cage, is replaced by Ser129 in PP1, leading to much diminished capacity in mediating van der Waals interaction. The net effect of these substitutions is that PP1 contains an open-ended groove, whereas PP2A possesses a hydrophobic cage that better accommodates the hydrophobic end of OA [48].

4.1.3. The Current Pharmacophore for Phosphatase Inhibition of OA and its Challenge

The interactions observed from the X-ray structures of PP1·OA and PP2A·OA complexes are summarized in Fig. (**6**). A total of six elements in OA, including an acidic group, a proximal methyl group, two hydrogen bonding sites, β12-β13 loop-contacting region, and a hydrophobic tail group, are proposed as the pharmacophore for phosphatase inhibition. The key elements of the pharmacophore for potent phosphatase inhibition are the acidic group, the β12-β13 loop-contacting region, a hydrogen bonding site, and the hydrophobic tail group (see Fig. **6**) [48]. Perhaps the most critical features of the pharmacophore are the acidic group and the hydrophobic tail group.

Recently, two OA derivatives, 19-*epi*-OA (**2**) and belizeanic acid (**26**), have been identified from the marine dinoflagellate *P. belizeanum* [10, 24]. The former has the opposite absolute configuration at C-19 to that of OA and the latter is the OA derivative with the opening of rings C and D. The comparison of the conformations in solution of OA versus 19-*epi*-OA shows a major difference. While OA shows a right-hand twist, 19-*epi*-OA turns in the opposite direction, thus preventing the formation of the C-24/C-1 hydrogen bond. However, 19-*epi*-OA potentially inhibits PP2A equipotent to OA and its selectivity for PP2A versus PP1 surpasses that shown by OA 10-fold. This can not be interpreted only on the basis of the pharmacophore proposed by the aforementioned OA-PP1/PP2A complexes [10]. However, despite the opening of two rings, belizeanic acid still turns out to be a potent PP1 inhibitor. Its inhibitory activity versus PP1 shows a slight loss of activity relative to OA. Bioassays *in vitro* revealed that belizeanic acid presented an IC_{50} of 318 ± 37 nM, whereas OA showed an IC_{50} of 62 ± 6 nM. The results of molecular docking calculations for belizeanic acid and PP1 active site complex suggested that the possible interactions between them might be different from those found in the aforementioned OA-PP1/PP2A complexes [24].

4.2. Cellular Effects of OA and Methyl OA

Two phosphatases, PP1 and PP2A, account for more than 90% of total protein serine/threonine phosphatase activity in mammalian cells. PP1 appears to play a key role in the regulation of glycogen metabolism, smooth muscle contraction, cell division, and protein synthesis, whereas PP2A participates in the control of most major metabolic pathways such as glycolysis and lipid metabolism, apoptosis, cell growth and division, gene transcription, and protein synthesis [49]. Due to its mechanism of action and selectivity, OA can be used to differentiate those cellular processes that involve phosphorylation steps mediated by PP1 and/or PP2A. As a consequence, OA has been extensively used in the past years as a tool to understand and control the cell cycle, to research on the action mechanism of apoptosis, tumour promotion, glycogen synthesis, and effects on smooth muscle contraction [49].

Recently, confocal microscopy imaging has revealed that methyl OA (**21**) induces reorganization of actin cytoskeleton, with loss of the typical flattened morphology, adoption of a round shape, and a reduction in the number of neurites. The potency induced by methyl OA is approximately 10-fold lower than that by OA. It is found that methyl OA induces an increase of Ser/Thr phosphorylation of cellular proteins detected by western blot, showing similar phosphorylation profiles to OA. These results suggest that methyl OA shares a pharmacological target that may be a Ser/Thr phosphatase with OA. However, it is probably different from PP1 and PP2A [50].

5. CONCLUDING REMARKS AND PERSPECTIVES

To date, twenty-six OA analogues have been identified from dinoflagellates of the genus *Prorocentrum*. Biosynthetic origin studies of OA and its analogues reveal that these DSP toxins are biosynthesized *via* a polyketide pathway. The pharmacophore for phosphatase inhibition of OA to PP1 and PP2A is disclosed by the analysis of X-ray structure of their complexes. However, recent discovery of two OA derivatives, 19-*epi*-OA and belizeanic acid from *P. belizeanum*,

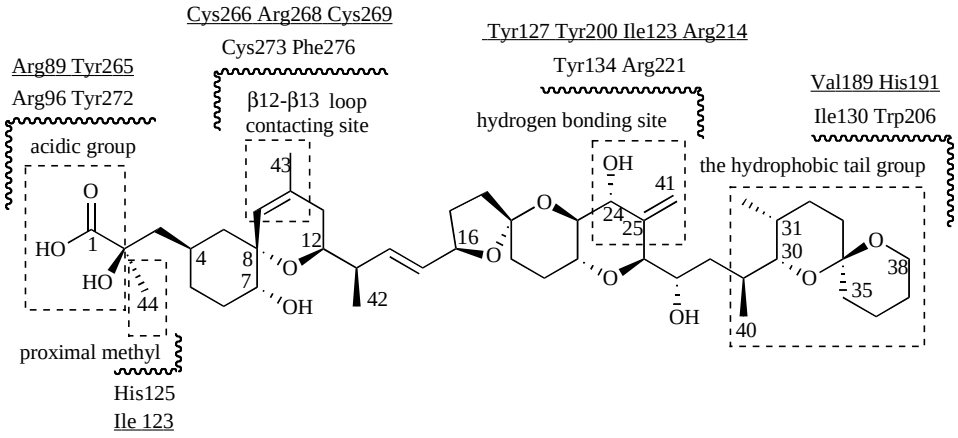

Fig. (6). Okadaic acid with the features of the pharmacophore highlighted and the key PP1 and PP2A contacting residues depicted according to X-ray complex (underlined residues are from the catalytic subunit of PP2A).

and their potent phosphatase inhibitory activities to PP1 or PP2A, challenges the current pharmacophore models.

Different *Prorocentrum* species can produce different OA derivatives with different substituents or conformational change on their skeleton. The isolation and characterization of polyketides from these dinoflagellates may lead to the discovery of many novel OA analogues with phosphatase inhibitory activity. The structure-activity relationships between OA / PP1 and OA / PP2A will be deeply understood in the future after creating sufficient molecular diversity of OA derivates by way of natural products isolation and chemical synthesis.

Since genomes of most dinoflagellates are large, the discovery of the polyketide biosynthetic gene clusters for OA from *Prorocentrum* species is difficult. However, the genome-wide approaches will lead to the identification of these gene clusters in the future. Eventually, there will come a time when genome sequencing will become practical for these dinoflagellates. Demand for novel polyketides from dinoflagellates in uses as medicinal leads, molecular tools, and in understanding toxin biosynthesis, will continue to drive the research in this field.

6. ACKNOWLEDGEMENTS

We thank every author of all the references cited herein for their valuable contributions. Financial support for this work from the Important Project of Chinese Academy of Sciences (KSCX2-YW-R-093) and the National High Technology Research and Development Program of China (863 Program) (2007AA09Z407) is gratefully acknowledged.

7. REFERENCES

[1] Tachibana, K.; Scheuer, P. J.; Tsukitani, Y.; Kikuchi, H.; Van Engen, D.; Clardy, J.; Gopichand, Y.; Schmitz, F. J. Okadaic acid, a cytotoxic polyether from two marine sponges of the genus *Halichondria*. *J. Am. Chem. Soc.*, **1981**, *103*, 2469-71.

[2] Schmitz, F. J.; Prasad, R. S.; Gopichand, Y.; Hossain, M. B.; Van der Helm, D.; Schmidt, P. Acanthifolicin, a new episulfide-containing polyether carboxylic acid from extracts of the marine sponge *Pandaros acanthifolium*. *J. Am. Chem. Soc.*, **1981**, *103*, 2467-9.

[3] Murakami, Y.; Oshima, Y.; Yasumoto, T. Identification of okadaic acid as a toxic component of a marine dinoflagellate *Prorocentrum lima*. *Bull. Jpn. Soc. Sci. Fish.*, **1982**, *48*, 69-72.

[4] Hu, T. M.; Marr, J.; Defreitas, A. S. W.; Quilliam, M. A.; Walter, J. A.; Wright, J. L. C.; Pleasance, S. New diol esters isolated from cultures of the dinoflagellates *Prorocentrum lima* and *Prorocentrum concavum*. *J. Nat. Prod.*, **1992**, *55*, 1631-7.

[5] Morton, S. L. Morphology and toxicology of *Prorocentrum faustiae sp*. nov., a toxic species of non-planktonic dinoflagellate from Heron Island, Australia. *Bot. Mar.*, **1998**, *41*, 565-9.

[6] Ten-Hage, L.; Delaunay, N.; Pichon, V.; Coute, A.; Puiseux-Dao, S.; Turquet, J. Okadaic acid production from the marine benthic dinoflagellate *Prorocentrum arenarium* Faust (Dinophyceae) isolated from Europa Island coral reef ecosystem (SW Indian Ocean). *Toxicon*, **2000**, *38*, 1043-54.

[7] Cruz, P. G.; Daranas, A. H.; Fernandez, J. J.; Souto, M. L.; Norte, M. DTX5c, a new OA sulphate ester derivative from cultures of *Prorocentrum belizeanum*. *Toxicon*, **2006**, *47*, 920-4.

[8] Dickey, R. W.; Bobzin, S. C.; Faulkner, D. J.; Bencsath, F. A.; Andrzejewski, D. Identification of okadaic acid from a Caribbean dinoflagellate, Prorocentrum concavum. *Toxicon*, **1990**, *28*, 371-7.

[9] Cruz, P. G.; Daranas, A. H.; Fernandez, J. J.; Norte, M. 19-epi-okadaic acid, a novel protein phosphatase inhibitor with enhanced selectivity. *Org. Lett.*, **2007**, *9*, 3045-8.

[10] Marr, J. C.; Jackson, A. E.; Mclachlan, J. L. Occurrence of *Prorocentrum lima*, a DSP toxin-producing species from the Atlantic coast of Canada. *J. Appl. Phycol.*, **1992**, *4*, 17-24.

[11] Bravo, I.; Fernandez, M. L.; Ramilo, I.; Martinez, A. Toxin composition of the toxic dinoflagellate *Prorocentrum lima* isolated from different locations along the Galician coast (NW Spain). *Toxicon*, **2001**, *39*, 1537-45.

[12] Hu, T. M.; Curtis, J. M.; Walter, J. A.; Wright, J. L. C. Identification of DTX-4, a new water-soluble phosphatase inhibitor from the toxic dinoflagellate *Prorocentrum lima*. *J. Chem. Soc. Chem.Commun.*, **1995**, 597-9.

[13] Nascimento, S. M.; Purdie, D. A.; Morris, S. Morphology, toxin composition and pigment content of *Prorocentrum lima* strains isolated from a coastal lagoon in southern UK. *Toxicon*, **2005**, *45*, 633-49.

[14] Hu, T.; Curtis, J. M.; Walter, J. A.; McLachlan, J. L.; Wright, J. L. C. Two New Water-soluble DSP toxin derivatives from the dinoflagellate *Prorocentrum maculosum*: possible storage and excretion products. *Tetrahedron Lett.*, **1995**, *36*, 9273-6.

[15] Suarez-Gomez, B.; Souto, M. L.; Norte, M.; Fernandez, J. J. Isolation and structural determination of DTX-6, a new okadaic acid derivative. *J. Nat. Prod.*, **2001**, *64*, 1363-4.

[16] Fernandez, J. J.; Suarez-Gomez, B.; Souto, M. L.; Norte, M. Identification of new okadaic acid derivatives from laboratory cultures of *Prorocentrum lima*. *J. Nat. Prod.*, **2003**, *66* (9), 1294-6.

[17] Suarez-Gomez, B.; Souto, M. L.; Cruz, P. G.; Fernandez, J. J.; Norte, M. New targets in diarrhetic shellfish poisoning control. *J. Nat. Prod.*, **2005**, *68*, 596-9.

[18] Yasumoto, T.; Murata, M.; Lee, J.; Torigoe, K. In *Mycotoxins and Phycotoxins '88*, Natori, S.; Hashimoto, K.; Ueno, Y., Ed.; Elsevier Science Publishers: Amsterdam, **1989**, pp. 375-82.

[19] Yasumoto, T.; Seino, N.; Murakami, Y.; Murata, M. Toxins produced by benthic dinoflagellates. *Biol. Bull.*, **1987**, *172*, 128-31.

[20] Nagai, H.; Satake, M.; Yasumoto, T. Antimicrobial activities of polyether compounds of dinoflagellate origins. *J. Appl. Phycol.*, **1990**, *2*, 305-8.

[21] Norte, M.; Padilla, A.; J. Fernandez, J.; L. Souto, M. Structural determination and biosynthetic origin of two ester derivatives of okadaic acid isolated from *Prorocentrum lima*. *Tetrahedron*, **1994**, *50*, 9175-80.

[22] Schmitz, F. J.; Yasumoto, T. The 1990 United States-Japan seminar on bioorganic marine chemistry, meeting report. *J. Nat. Prod.*, **1991,** *54*, 1469-90.

[23] Holmes, M. J.; Lee, F. C.; Khoo, H. W.; Teo, S. L. M. Production of 7-deoxy-okadaic acid by a new caledonian strain of *Prorocentrum lima* (Dinophyceae). *J. Phycol.*, **2001**, *37*, 280-8.

[24] Cruz, P. G.; Fernandez, J. J.; Norte, M.; Daranasa, A. H., Belizeanic acid: A potent protein phosphatase 1 inhibitor belonging to the okadaic acid class, with an unusual skeleton. *Chem. Eur. J.*, **2008**, *14*, 6948-56.

[25] Terao, K.; Ito, E.; Yanagi, T.; Yasumoto, T. Histopathological studies on experimental marine toxin poisoning. Ultrastructural-changes in the small-intestine and liver of suckling mice induced by dinophysistoxin-1 and pectenotoxin-11. *Toxicon*, **1986**, *24*, 1141-51.

[26] Yasumoto, T.; Murata, M. *Polyether toxins involved in seafood poisoning*. In *Marine Toxins: Origin, structure and molecular pharmacology*, Hall, S. and Strichartz, G., Ed.; American Chemical Society, **1990**; pp. 120-32.

[27] Aune, T.; Larsen, S.; Aasen, J. A. B.; Rehmann, N.; Satake, M.; Hess, P. Relative toxicity of dinophysistoxin-2 (DTX-2) compared with okadaic acid, based on acute intraperitoneal toxicity in mice. *Toxicon*, **2007**, *49*, 1-7.

[28] Torigoe, K.; Murata, M.; Yasumoto, T.; Iwashita, T. Prorocentrolide, a toxic nitrogenous macrocycle from a marine dinoflagellate, *Prorocentrum lima*. *J. Am. Chem. Soc.*, **1988**, *110*, 7876-7.

[29] Torigoe, K. Structure and biosynthesis of bioactive substances produced by the dinoflagellate *Prorocentrum lima*. Tohoku University: Sendai, **1990**.

[30] Lu, C.-K.; Lee, G.-H.; Huang, R.; Chou, H.-N. Spiro-prorocentrimine, a novel macrocyclic lactone from a benthic *Prorocentrum sp*. of Taiwan. *Tetrahedron Lett.*, **2001**, *42*, 1713-6.

[31] Hu, T.; deFreitas, A. S. W.; Curtis, J. M.; Oshima, Y.; Walter, J. A.; Wright, J. L. C. Isolation and structure of prorocentrolide b, a

fast-acting toxin from *Prorocentrum maculosum*. *J. Nat. Prod.*, **1996**, *59*, 1010-4.

[32] Hu, T.; Curtis, J. M.; Walter, J. A.; Wright, J. L. C. Hoffmanniolide: a novel macrolide from *Prorocentrum hoffmannianum*. *Tetrahedron Lett.*, **1999**, *40*, 3977-80.

[33] Lu, C. K.; Chou, H. N.; Lee, C. K.; Lee, T. H. Prorocentin, a new polyketide from the marine dinoflagellate *Prorocentrum lima*. *Org. Lett.*, **2005**, *7* (18), 3893-6.

[34] Napolitano, J. G.; Norte, M.; Padron, J. M.; Fernandez, J. J.; Daranas, A. H. Belizeanolide, a cytotoxic macrolide from the dinoflagellate *Prorocentrum belizeanum*. *Angew. Chem. Int. Ed.*, **2009**, *48*, 796-9.

[35] Norte, M.; Padilla, A.; Fernandez, J. J. Studies on the biosynthesis of the polyether marine toxin di nophysistoxin-1 (DTX-1). *Tetrahedron Lett.*, **1994**, *35*, 1441-4.

[36] Needham, J.; Mclachlan, J. L.; Walter, J. A.; Wright, J. L. C. Biosynthetic origin of C-37 and C-38 in the polyether toxins okadaic acid and dinophysistoxin-1. *J. Chem. Soc. Chem. Commun.*, **1994**, 2599-600.

[37] Daranas, A. H.; Fernández, J. J.; Norte, M.; Gavín, J. A.; Suárez-Gómez, B.; Souto, M. L. Biosynthetic studies of the DSP toxin skeleton. *Chem. Rec.*, **2004**, *4*, 1-9.

[38] Murata, M.; Izumikawa, M.; Tachibana, K.; Fujita, T.; Naoki, H. Labeling pattern of okadaic acid from $^{18}O_2$ and [$^{18}O_2$]acetate elucidated by collision-induced dissociation tandem mass spectrometry. *J. Am. Chem. Soc.*, **1998,** *120*, 147-51.

[39] Izumikawa, M.; Murata, M.; Tachibana, K.; Fujita, T.; Naoki, H. ^{18}O-labelling pattern of okadaic acid from $h_2{}^{18}o$ in dinoflagellate *Prorocentrum Lima* elucidated by tandem mass spectrometry. *Eur. J. Biochem.*, **2000**, *267*, 5179-83.

[40] Wright, J. L. C.; Hu, T.; McLachlan, J. L.; Needham, J.; Walter, J. A. Biosynthesis of DTX-4: confirmation of a polyketide pathway, proof of a Baeyer-Villiger oxidation step, and evidence for an unusual carbon deletion process. *J. Am. Chem. Soc.*, **1996**, *118*, 8757-8.

[41] Macpherson, G. R.; Burton, I. W.; LeBlanc, P.; Walter, J. A.; Wright, J. L. Studies of the biosynthesis of DTX-5a and DTX-5b by the dinoflagellate *Prorocentrum maculosum*: regiospecificity of the putative Baeyer-Villigerase and insertion of a single amino acid in a polyketide chain. *J. Org. Chem.*, **2003**, *68*, 1659-64.

[42] Bialojan, C.; Takai, A. Inhibitory effect of a marine-sponge toxin, okadaic acid, on protein phosphatases: specificity and kinetics. *Biochem. J.*, **1988**, *256*, 283-90.

[43] Haystead, T. A. J.; Sim, A. T. R.; Carling, D.; Honnor, R. C.; Tsukitani, Y.; Cohen, P.; Hardie, D. G. Effects of the tumour promoter okadaic acid on intracellular protein phosphorylation and metabolism. *Nature*, **1989**, *337*, 78-81.

[44] Cohen, P.; Klumpp, S.; Schelling, D. L. An Improved procedure for identifying and quantitating protein phosphatases in mammalian-tissues. *FEBS Lett.*, **1989**, *250*, 596-600.

[45] Villafranca, J. E.; Kissinger, C. R.; Parge, H. E. Protein serine/threonine phosphatases. *Curr. Opin. Biotechnol.*, **1996**, *7*, 397-402.

[46] Maynes, J. T.; Bateman, K. S.; Cherney, M. M.; Das, A. K.; Luu, H. A.; Holmes, C. F. B.; James, M. N. G. Crystal structure of the tumor-promoter okadaic acid bound to protein phosphatase-1. *J. Biol. Chem.*, **2001**, *276*, 44078-82.

[47] Xing, Y.; Xu, Y.; Chen, Y.; Jeffrey, P. D.; Chao, Y.; Lin, Z.; Li, Z.; Strack, S.; Stock, J. B.; Shi, Y. Structure of protein phosphatase 2A core enzyme bound to tumor-inducing toxins. *Cell*, **2006**, *127*, 341-53.

[48] Colby, D. A.; Chamberlin, A. R. Pharmacophore identification: The case of the Ser/Thr protein phosphatase inhibitors. *Mini-Rev. Med. Chem.* **2006**, *6*, 657-65.

[49] Fernandez, J. J.; Candenas, M. L.; Souto, M. L.; Trujillo, M. M.; Norte, M. Okadaic acid, useful tool for studying cellular processes. *Curr. Med. Chem.*, **2002**, *9*, 229-62.

[50] Vilarino, N.; Ares, I. R.; Cagide, E.; Louzao, M. C.; Vieytes, M. R.; Yasumoto, T.; Botana, L. M. Induction of actin cytoskeleton rearrangement by methyl okadaate-comparison with okadaic acid. *FEBS J.*, **2008**, *275*, 926-34.

Received: August 15, 2009 Revised: October 22, 2009 Accepted: October 23, 2009